

# *B*-Mode contamination by synchrotron emission from 3-years WMAP data

E. Carretti<sup>1\*</sup>, G. Bernardi<sup>2</sup>, and S. Cortiglioni<sup>3</sup>

<sup>1</sup>*INAF – Istituto di Radioastronomia, Via Gobetti 101, I-40129 Bologna, Italy*

<sup>2</sup>*Kapteyn Astronomical Institute, University of Groningen, PO BOX 800, 9700, AV Groningen, The Netherlands*

<sup>3</sup>*INAF – IASF Bologna, Via Gobetti 101, Bologna, I-40129, Italy*

Accepted xx xx xx. Received yy yy yy; in original form zz zz zz

## ABSTRACT

We study the contamination of the *B*-mode of the Cosmic Microwave Background Polarization (CMBP) by Galactic synchrotron in the lowest emission regions of the sky. The 22.8-GHz polarization map of the 3-years WMAP data release is used to identify and analyse such regions. Two areas are selected with signal-to-noise ratio  $S/N < 2$  and  $S/N < 3$ , covering  $\sim 16\%$  and  $\sim 26\%$  fraction of the sky, respectively. The polarization power spectra of these two areas are dominated by the sky signal on large angular scales (multipoles  $\ell < 15$ ), while the noise prevails on degree scales. Angular extrapolations show that the synchrotron emission competes with the CMBP *B*-mode signal for tensor-to-scalar perturbation power ratio  $T/S = 10^{-3}$ – $10^{-2}$  at 70-GHz in the 16% lowest emission sky ( $S/N < 2$  area). These values worsen by a factor  $\sim 5$  in the  $S/N < 3$  region. The novelty is that our estimates regard the whole lowest emission regions and outline a contamination better than that of the whole high Galactic latitude sky found by the WMAP team ( $T/S > 0.3$ ). Such regions allow  $T/S \sim 10^{-3}$  to be measured directly which approximately corresponds to the limit imposed by using a sky coverage of 15%. This opens interesting perspectives to investigate the inflationary model space in lowest emission regions.

**Key words:** cosmology: cosmic microwave background – polarization – radio continuum: ISM – cosmology: diffuse radiation – radiation mechanisms: non-thermal.

## 1 INTRODUCTION

The Cosmic Microwave Background Polarization (CMBP) allows the study of the first stages of the Universe and is one of the hot topics of cosmology. One of its components, the *B*-mode, is sensitive to the primordial Gravitational Wave (GW) background left by inflation giving a way to investigate the physics of the very early Universe (e.g. Kamionkowski & Kosowsky 1998). In fact, its power spectrum on degree scales has a linear dependence on the tensor-to-scalar perturbation power ratio  $T/S$ , which measures the amount of primordial GW (e.g. Boyle et al. 2006; Kinney et al. 2006). In combination with parameters measured by the CMB Temperature spectrum (the scalar perturbation spectral index  $n$  and its running  $dn/d \ln k$ ), it allows us to distinguish among the numerous models of inflation.

The *B*-mode signal is faint and only upper limits of  $T/S$  have been set so far. Seljak et al. (2006) and Martin & Ringeval (2006), using different analyses, find consistent results of  $T/S < 0.22$  and  $T/S < 0.21$  (95% C.L.),

respectively. On the other hand, the plethora of inflation models does not help constrain  $T/S$ . This can vary by orders of magnitude and can be even smaller than  $10^{-4}$ , although Boyle et al. (2006) show that only models with high fine tuning degree can feature  $T/S < 10^{-3}$ . Correspondingly, the peak *B*-mode signal can vary from  $\sim 200$  nK of the present upper limits down to values even smaller than 3 nK for  $T/S < 10^{-4}$ .

The weakness of the CMB *B*-mode makes it easily contaminated by foreground emissions from both the Galaxy and extragalactic sources. The study of astrophysical foregrounds is thus crucial to set the capability of CMBP experiments to investigate the early Universe and help set which part of the inflationary model space is accessible.

At frequencies lower than 60–70 GHz, the most relevant contaminant is expected to be the Galactic synchrotron emission. Recent results based on 3-years Wilkinson Microwave Anisotropy Probe (WMAP) data at 22.8-GHz show that even the high Galactic latitudes are normally strongly contaminated (Page et al. 2006). These authors use about 75 percent of the sky (all high latitudes but strong large local structures like the Northern Galactic Spur) and find

\* E-mail: carretti@ira.inaf.it

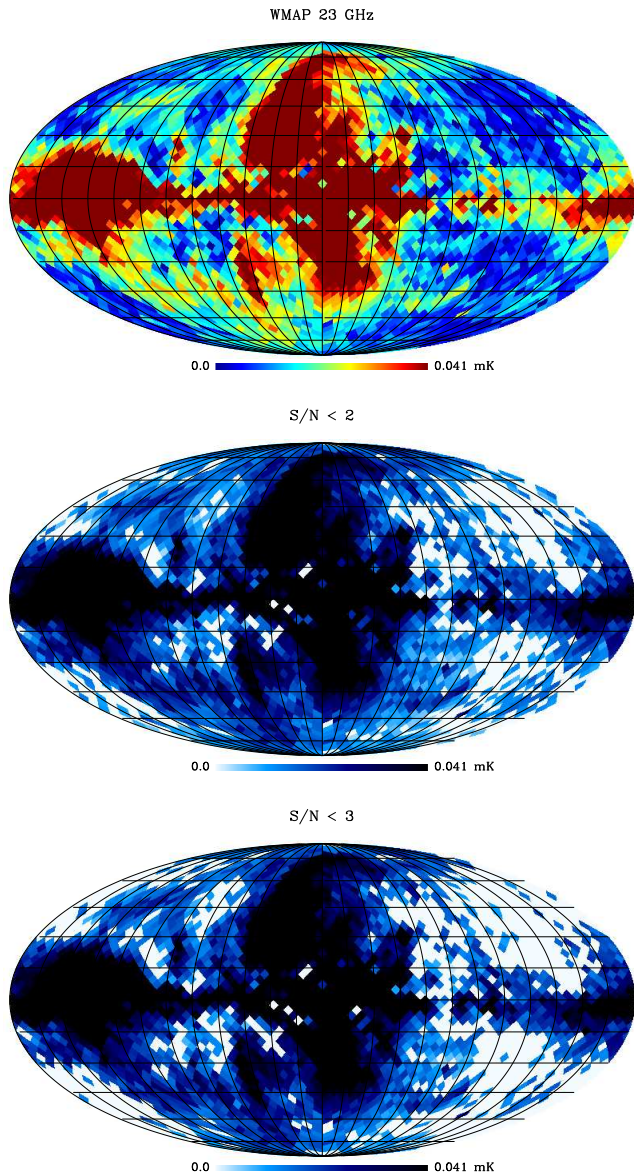


**Figure 1.** *Top.* Polarized intensity map at 22.8-GHz of the WMAP experiment (Page et al. 2006). Data are averaged on  $\sim 4^\circ$  scale using the HEALPix (Górski et al. 2005) pixelation with parameter  $N_{\text{side}} = 16$  (resolution r4). The map is in Galactic coordinates with the Galactic centre in the middle. The coordinate grid is  $15^\circ$  spaced both in longitude and latitude. Lowest emission regions are the blue spots at mid-high Galactic latitudes out of the large SNR loops. *Mid and bottom.* Lowest emission regions in the 22.8-GHz WMAP polarization map: the  $4^\circ$ -pixels of the two regions with  $S/N < 2$  (mid) and  $S/N < 3$  (bottom) are blanked (white).

that at 60–70 GHz the synchrotron emission competes with the cosmic  $B$ -mode signal even for models with  $T/S = 0.3$ – $0.5$ , which are already disfavoured by the present upper limits. Similar results are obtained by La Porta et al. (2006) through the analysis of the 1.4 GHz sky at latitude  $|b| > 20^\circ$  using the DRAO survey data (Wolleben et al. 2006).

La Porta et al. (2006) also analyse areas<sup>1</sup> with smaller extension (for a total of about 10% of the sky) and lower emission, finding that the Galactic signal at 70-GHz is comparable to the CMB  $B$ -mode in case of  $T/S \sim 0.1$ . Even though lower, this signal would largely contaminate the CMB  $B$ -mode for most of the  $T/S$  values presently allowed. However, these areas are not in the lowest emission regions visible in the 22.8-GHz WMAP polarization map.

Information about the lowest emission regions are available, instead, from three independent small areas observed at 1.4 and 2.3-GHz (Carretti et al. 2005b, 2006; Bernardi et al. 2006). The synchrotron emission here actually looks weaker, competing with the CMB  $B$ -mode only for cosmological models with  $T/S = 10^{-3}$ – $10^{-2}$  at 70-GHz (Carretti et al. 2006).

Such values would give more chances to investigate a large part of the inflationary model space, opening interesting perspective for the study of the inflation physics. However, the areas observed so far cover just few square degrees ( $\sim 20\text{-deg}^2$  in total) and represent few sparse samples of the lowest emission regions. A real knowledge of the typical Galactic synchrotron contribution of such regions is still an open question, and requires wider areas to be analysed.

This paper reports the first study carried out to identify and analyse the areas with the lowest synchrotron emission at microwave wavelengths, which allow negligible Faraday rotation effects (still appreciable at  $\sim 1$ -GHz; e.g. see Carretti et al. 2005a). We use the 22.8-GHz polarization map of the 3-years WMAP data release to select them (Section 2), and compute their polarized angular power spectra (Section 3). Finally, we estimate the contamination of the CMBP by Galactic synchrotron in the CMBP frequency window (70–90 GHz) and discuss implications for the detection of the cosmic  $B$ -mode in lowest emission regions (Section 4).

## 2 LOWEST EMISSION REGIONS SELECTION

The 3-years WMAP data release<sup>2</sup> has made available the first polarization all-sky map at microwave frequencies, namely 22.8-GHz (Page et al. 2006). The sensitivity does not allow to detect the signal out of the Galactic plane at the nominal resolution (FWHM  $\sim 1^\circ$ ). The high Galactic latitudes have low signal-to-noise ratios ( $S/N$ ), except in large local structures like the big Supernova Remnant (SNR) loops. The situation improves once data are averaged on pixels of  $\sim 4^\circ$  (top panel of Figure 1), as presented by the WMAP team (Page et al. 2006). At this resolution the signal appears even at high Galactic latitudes and allows us to identify the lowest emission regions in the sky (blue areas in top panel of Figure 1), which, however, still have signal competing with the noise.

We quantitatively select the lowest emission regions using the  $4^\circ$  polarized intensity map. After accounting for the noise bias (Uyaniker & Landecker 2002), pixels with  $S/N$  smaller than a given threshold have been selected. Namely,

<sup>1</sup> Three areas defined as follows: A)  $180^\circ < l < 276^\circ$ ,  $b > 45^\circ$ ; B)  $193^\circ < l < 228^\circ$ ,  $b < -45^\circ$ ; C)  $65^\circ < l < 180^\circ$ ,  $b > 45^\circ$ ;  $l$  and  $b$  are Galactic longitude and latitude.

<sup>2</sup> <http://lambda.gsfc.nasa.gov/>

we have considered two values:  $S/N < 2$  and  $S/N < 3$ . The two resulting regions are shown in Figure 1.

These regions are not contiguous and located at mid-high Galactic latitudes, mainly in the third Galactic quadrant, with significant extensions in the second one. It is worth noting that the Galactic caps are not included, having too high emission.

The sky fractions covered are 16.2% ( $S/N < 2$ ) and 25.7% ( $S/N < 3$ ), respectively. Although smaller than half a sky, these two regions have significant extensions and could still effectively be used for CMBP  $B$ -mode studies.

### 3 POWER SPECTRUM ANALYSIS

We compute the  $E$ - and  $B$ -mode power spectra of the polarized emission in the two selected areas. These are the quantities predicted by cosmological models and allow a direct comparison with the CMBP signal.

To account for the irregular sky coverage we use the method based on two-point correlation functions of the Stokes parameters  $Q$  and  $U$  described by Sbarra et al. (2003). Correlation functions are estimated on the  $Q$  and  $U$  maps of the selected regions as

$$\tilde{C}^X(\theta) = X_i X_j \quad X = Q, U \quad (1)$$

where  $X_i$  is the pixel  $i$  content of map  $X$ ,  $i$  and  $j$  identify pixel pairs at distance  $\theta$ . Data are binned with pixel-size resolution. Power spectra  $C_\ell^{E,B}$  are obtained by integration

$$C_\ell^E + C_\ell^{E,n} = W_\ell \int_0^\pi [\tilde{C}^Q(\theta) F_{1,\ell 2}(\theta) + \tilde{C}^U(\theta) F_{2,\ell 2}(\theta)] \sin(\theta) d\theta \quad (2)$$

$$C_\ell^B + C_\ell^{B,n} = W_\ell \int_0^\pi [\tilde{C}^U(\theta) F_{1,\ell 2}(\theta) + \tilde{C}^Q(\theta) F_{2,\ell 2}(\theta)] \sin(\theta) d\theta \quad (3)$$

where the functions  $F_{1,\ell m}$  and  $F_{2,\ell m}$  are described by Zaldarriaga (1998),  $C_\ell^{E,n}$  and  $C_\ell^{B,n}$  are the noise spectra, and  $W_\ell$  is the pixel window function accounting for pixel smearing effects. The WMAP map smoothed on  $1^\circ$  pixels (HEALPix parameter  $N_{\text{side}} = 64$ ) has been used to compute correlation functions and spectra, instead of the  $4^\circ$  one used for the selection. This allows us to reduce the effects of the pixel window function and provides reliable computation up to  $\ell \sim 100$  of the  $B$ -mode peak.

Figure 2 shows  $B$ -mode spectra in the two selected areas. These are steep on large angular scales, with the  $S/N < 2$  case having less power than  $S/N < 3$ , as expected according to selection criteria. A flattening instead occurs on small angular scales. This behaviour indicates the signal prevails on large scales ( $\ell < 10$  and  $\ell < 15$  for  $S/N = 2$  and 3, respectively), while the noise dominates on smallest ones.

To check if the flat component is compatible with noise, we performed Montecarlo simulations. We have generated 100 noise map realizations assuming the sensitivity map provided in the WMAP data package. Then we compute their spectra using only the pixels of the two selected regions. For both the two cases, we find that the average spectrum is flat with normalization  $C_\ell^n = 7.5 \times 10^{-2} \mu\text{K}^2$  and  $7.3 \times 10^{-2} \mu\text{K}^2$  for  $S/N < 2$  and  $S/N < 3$ , respectively, which are compatible with the level of our spectra at large  $\ell$  (Figure 2). In addition, the spectra of the two  $S/N$  cases converge to the same value in the flat range, which again suggests the

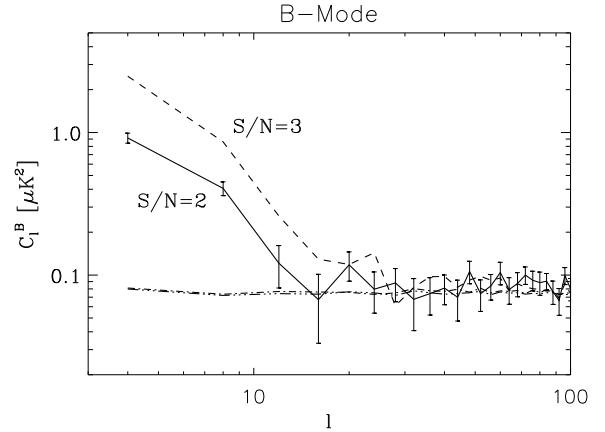


**Figure 2.**  $B$ -mode spectra of the WMAP 22.8-GHz polarization map in the two regions with  $S/N < 2$  (solid) and  $S/N < 3$  (dashed). To avoid confusion, error bars are reported for the  $S/N < 2$  case only. The mean noise spectra of the Montecarlo simulations are also reported (dot-dashed and triple-dot-dashed for  $S/N < 2$  and  $S/N < 3$ , respectively).

**Table 1.** Mean value of  $\langle \ell(\ell+1)/(2\pi)C_\ell^B \rangle$  – see text. Fit parameters of  $B$ -mode spectra for  $S/N < 3$  are also reported. The  $\ell$ -range used for the estimates is indicated.

$S/N$	$\ell$ -range	$A_{10}^B [\mu\text{K}^2]$	$\beta^B$	$\langle \frac{\ell(\ell+1)}{2\pi} C_\ell^B \rangle [\mu\text{K}^2]$
2	[4, 12]			$2.8 \pm 0.3$
3	[4, 24]	$0.30 \pm 0.06$	$-2.4 \pm 0.3$	$7.62 \pm 0.14$

spectra are noise dominated there. We use the mean noise spectra attained with the Montecarlo simulations to account for the noise bias in all the next evaluations.

We tried to fit a power law

$$C_\ell^B = A_{10}^B \left( \frac{\ell}{10} \right)^{\beta^B} \quad (4)$$

to the spectra. Only the case  $S/N < 3$  allows meaningful results (Table 1), because only few points (three) can be effectively used for  $S/N < 2$ , after the noise bias is subtracted for. To provide an estimate of the mean emission also for the  $S/N < 2$  case, we compute the mean value of the quantity  $\ell(\ell+1)/(2\pi)C_\ell^B$  over the usable  $\ell$ -range, which is  $\ell \leq 12$ . The result is reported in Table 1, along with the same estimate for the  $S/N < 3$  area. It is worth noting that there is a factor  $\sim 3$  in spectrum ( $\sim \sqrt{3}$  in signal) between the mean emissions of the two analysed regions. Moreover, the emission we found in the  $S/N < 2$  region is a factor  $\sim 10$  weaker than that measured in the  $\sim 75\%$  sky fraction in the same  $\ell$ -range (Page et al. 2006).

### 4 IMPLICATION FOR CMBP $B$ -MODE AND DISCUSSION

The contamination of the CMB  $B$ -mode signal can be estimated by extrapolating the spectra of Sect. 3 to 70-GHz, a frequency in the range where the combined contribution of synchrotron and dust is believed to be minimum (Page et al.

2006; Carretti et al. 2006). It is worth noting that typical values of rotation measure at high Galactic latitudes ( $RM \sim 10\text{--}20 \text{ rad m}^{-2}$ ) generate polarization angle rotations of 6–12 arcmin at 22.8-GHz. Thus, Faraday rotation effects can be considered negligible, allowing safe frequency extrapolations.

Our spectra are noise dominated at the multipole  $\ell$  the CMB  $B$ -mode peaks at ( $\ell \sim 90$ ) and a direct extrapolation of them would provide just upper limits. Then, we adopt another approach: we use the spectra measured in the  $\ell$ -range where they are signal-dominated and perform angular extrapolations to the scale of interest. The mean emission is that provided by the last column of Table 1. As for the extrapolation, the analysis of the 1.4-GHz DRAO survey data shows that the angular behaviour of Galactic synchrotron spectra is well represented by a power law

$$C_\ell \propto \ell^\beta \quad (5)$$

with slope  $\beta$  varying in the range  $[-2.5, -3.0]$  for  $\ell = 2\text{--}300$  (La Porta et al. 2006; Burigana et al. 2006). This is consistent with the value of  $\beta = -2.6$  quoted by the WMAP team for the whole 75% of the sky they consider (Page et al. 2006). We use as slope both the two edge values of the  $\beta$  range ( $-2.5$  and  $-3.0$ ) and start extrapolations from the middle of the  $\ell$ -range used to evaluate the mean spectrum, namely  $\ell_0 = 8, 14$  for  $S/N < 2, < 3$ , respectively.

Frequency extrapolations are performed assuming the brightness Temperature of the Galactic synchrotron follows a power law  $T_b^{\text{synch}} \propto \nu^\alpha$ , with  $\alpha = -3.1$  (Bernardi et al. 2004).

Results are reported in Figure 3. For the  $S/N < 2$  case, which concerns  $\sim 16\%$  of the sky, the contamination range covered by the two angular extrapolations at  $\ell \sim 90$  competes with the CMBP  $B$ -mode for models with  $T/S = [3 \times 10^{-3}, 1 \times 10^{-2}]$ . The comparison with previous measurements shows these values are significantly lower than the mean contamination estimated by the WMAP team for most of high Galactic latitudes. On the other hand, our results are similar to the contamination estimated in the small sky patches observed in low emission regions (Carretti et al. 2006 and references therein) giving a valuable consistency of results in regions selected with similar criteria (areas in lowest emission regions). Although with the uncertainties of an angular scale extrapolation, our results extend to the whole lowest emission regions the promising indications obtained in those few small sample areas covering just few square degrees, and strongly support the possibilities to access small  $T/S$  values in the lowest emission part of the sky.

The use of frequency slope  $\alpha = -3.1$  can be considered as a conservative approach. In fact, Hinshaw et al. (2006) fit the behaviour of the synchrotron total intensity, finding out a steepening of the slope at the highest frequencies of the WMAP range. In particular, they fit  $\alpha = -3.5$  in the range 23–60 GHz. With such a slope the synchrotron contamination at 70 GHz further reduces by a factor 2.5 with respect to  $\alpha = -3.1$  and even  $T/S \sim [1 \times 10^{-3}, 3 \times 10^{-3}]$  becomes accessible (yellow shaded area of Figure 3).

The situation is slightly worse for  $S/N < 3$ , as expected, since higher emission pixels are included in the analysis. However,  $T/S = [2 \times 10^{-2}, 4 \times 10^{-2}]$  looks still accessible even in this larger region, assuming  $\alpha = -3.1$ . These are values better than that for all the high Galactic lati-

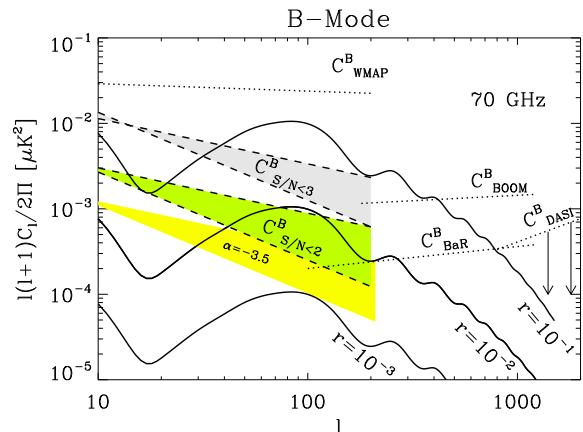


**Figure 3.**  $B$ -mode power spectra of the Galactic synchrotron emission estimated at 70-GHz in the regions with  $S/N < 2$  (green shaded area) and  $S/N < 3$  (gray shaded area). The two angular extrapolations with  $\beta = -2.5$  and  $-3.0$  are reported (upper and lower dashed line of shaded areas). A slope  $\alpha = -3.1$  is assumed for the frequency extrapolation. The case of a slope  $\alpha = -3.5$  is also reported for the  $S/N < 2$  region (yellow shaded). For comparison, the plot shows CMB spectra for three different values of  $r = T/S$ , the synchrotron emission detected in the two low emission areas in the target fields of the BOOMERanG ( $C_{\text{BOOM}}^B$ , Carretti et al. 2005b) and BaR-SPOrt experiments ( $C_{\text{BaR}}^B$ , Carretti et al. 2006), and the upper limit found in the DASI fields ( $C_{\text{DASI}}^B$ , Bernardi et al. 2006). Finally, the general contamination at high Galactic latitude, as estimated by the WMAP team using 74.3% of the sky is also reported: the spectrum at 22.8-GHz is considered (Page et al. 2006) and extrapolated to 70-GHz.

tudes (WMAP results on  $\sim 75\%$  of the sky), or in the areas analysed by La Porta et al. (2006).

For the lowest emission areas, the minimum combined synchrotron-dust contamination has been found to be somewhere between 70 and 90-GHz (Carretti et al. 2006). It is thus worthy estimating the synchrotron contamination of our best case ( $S/N < 2$ ) even at 90-GHz. A further factor  $\sim 4$  is gained with respect to 70-GHz (in thermodynamic temperature), and the Galactic signal competes with models with  $T/S \sim [1 \times 10^{-3}, 3 \times 10^{-3}]$ .

Despite the significant general contamination of high Galactic latitudes, the results obtained by our analysis depict a situation with better and interesting conditions in the lowest emission regions. The possibility to reach  $T/S$  values as low as  $10^{-3}\text{--}10^{-2}$  looks now extended from few small good sky patches to an area representing  $\sim 16\%$  of the sky, that could be the right place for deep CMBP observations looking at the  $B$ -mode.

To limit observations in small regions, however, imposes intrinsic constraints on the minimum detectable  $T/S$ , mainly because of the leakage from  $E$ - into the weaker  $B$ -mode. In fact, Amarie et al. (2005) find that an all-sky survey would allow a detection of  $T/S$  with a theoretical sensitivity limit of  $\Delta(T/S) = 1.5 \times 10^{-5}$ , that becomes  $\Delta(T/S) = 3.2 \times 10^{-5}$  when 70% of the sky is available, and  $\Delta(T/S) = 10^{-3}$  for 15% ( $3\text{-}\sigma$  C.L.). It is worth noting that the class of inflationary models with minimal fine-tuning have  $T/S$  values ranging within  $10^{-3}$  and  $10^{-1}$  (Boyle et al.

2006), for which a 15% sky portion would be large enough for the first detection of the tensor CMBP component.

In spite of these limitation, the minimum  $T/S$  value detectable in 15% of the sky almost matches the limit imposed by the foregrounds we have found in lowest emission regions. Although the uncertainties because of the angular extrapolations we need to apply, the search for the  $B$ -mode in a sky portion of such a size could thus be a good trade-off between intrinsic and foregrounds limits.

In addition, the weakness of the  $B$ -mode signal makes already a challenge to detect the signal for  $T/S = 0.1$  with the present technology (e.g. Cortiglioni & Carretti 2006). It is likely that significant technological improvements will be necessary before cosmologists can face an all-sky mapping mission with a sensitivity able to match the intrinsic limit of  $\Delta(T/S) \sim 10^{-5}$ . Therefore, an experiment aiming at detecting the  $B$ -mode in a smaller region (10-15% of the sky) can be a valuable intermediate step that would allow us to probe inflation models down to  $T/S = 10^{-3}$ .

## ACKNOWLEDGMENTS

We thank an anonymous referee for valuable comments, which helped improve the paper. Some of the results in this paper have been derived using the HEALPix package (<http://healpix.jpl.nasa.gov>). We acknowledge the use of the CMBFAST package, WMAP data, and the Legacy Archive for Microwave Background Data Analysis (LAMBDA). Support for LAMBDA is provided by the NASA Office of Space Science.

## REFERENCES

- Amarie M., Hirata C., & Seljak U., 2005, Physical Review D, 72, id. 123006
- Bernardi G., Carretti E., Fabbri R., Sbarra C., Poppi S., Cortiglioni S., Jonas J.L., 2004, MNRAS, 351, 436
- Bernardi G., Carretti E., Sault R.J., Cortiglioni S., Poppi S., 2006, MNRAS, 370, 2064
- Boyle L.A., Steinhardt P.J., & Turok N., 2006, Phys. Rev. Lett. 96, 111301
- Burigana C., La Porta L., Reich P., Reich W., 2006, Astron. Nachr., 327, 491
- Carretti E., Bernardi G., Sault R.J., Cortiglioni S., & Poppi S., 2005a, MNRAS, 358, 1
- Carretti E., McConnell D., McClure-Griffiths N.M., Bernardi G., Cortiglioni S., & Poppi S., 2005b, MNRAS, 360, L10
- Carretti E., Poppi S., Reich W., Reich P., Fürst E., Bernardi G., Cortiglioni S., Sbarra C., 2006, MNRAS, 367, 132
- Cortiglioni S., & Carretti E., 2006, in Fabbri R. ed., Cosmic Polarization, in press, astro-ph/0604169
- Górski K.M., et al., 2005, ApJ, 622, 759
- Hinshaw G., et al., 2006, ApJ, submitted, astro-ph/0603451
- Kamionkowski M., Kosowsky A., 1998, PRD, 57, 685
- Kinney W.H., Kolb E.W., Melchiorri A., & Riotto A., 2006, astro-ph/0605338
- La Porta L., Burigana C., Reich W., Reich P., 2006, A&A Letters, in press, astro-ph/0607300
- Martin J., Ringeval C., 2006, JCAP, in press, astro-ph/0605367
- Page L., et al., 2006, ApJ, submitted, astro-ph/0603450
- Sbarra C., Carretti E., Cortiglioni S., Zannoni M., Fabbri R., Macculi C., Tucci M., 2003, A&A, 401, 1215
- Seljak U., Slosar A., McDonald P., 2006, astro-ph/0604335
- Uyaniker B., Landecker T.L., 2002, ApJ, 575, 225
- Wolleben M., Landecker T.L., Reich W., & Wielebinski R., 2006, A&A, 448, 411
- Zaldarriaga M., 1998, Ph.D. Thesis, M.I.T., astro-ph/9806122

This paper has been typeset from a  $\text{\TeX}$ / $\text{\LaTeX}$  file prepared by the author.